

A perspective of superconductivity as multiband phenomena: Cuprate, iron and aromatic systems

Hideo Aoki

*Department of Physics,
University of Tokyo, Hongo,
Tokyo 113-0033, Japan
aoki@phys.s.u-tokyo.ac.jp*

Abstract

A theoretical overview of the classes of superconductors encompassing (a) high-T_c cuprate, (b) iron-based and (c) aromatic superconductors is given. Emphasis is put on the multiband natures of all the three classes, where the differences in the multiorbits and their manifestations in the electronic structures and pairing are clarified. From these, future directions and prospects are discussed.

INTRODUCTION

At the occasion of the centenary of the discovery of superconductor, it is meaningful to give an overview of different classes of superconductors, which have been discovered in recent decades. I shall do this theoretically for the three classes of superconductors, namely (a) high- T_c cuprate[1], (b) iron-based[2–4] and (c) aromatic superconductors[5, 6] (Fig.1). The purpose is two-fold: we can first look at the commonalities and differences among these classes of materials. We can then discuss future directions and prospects for the coming decades.

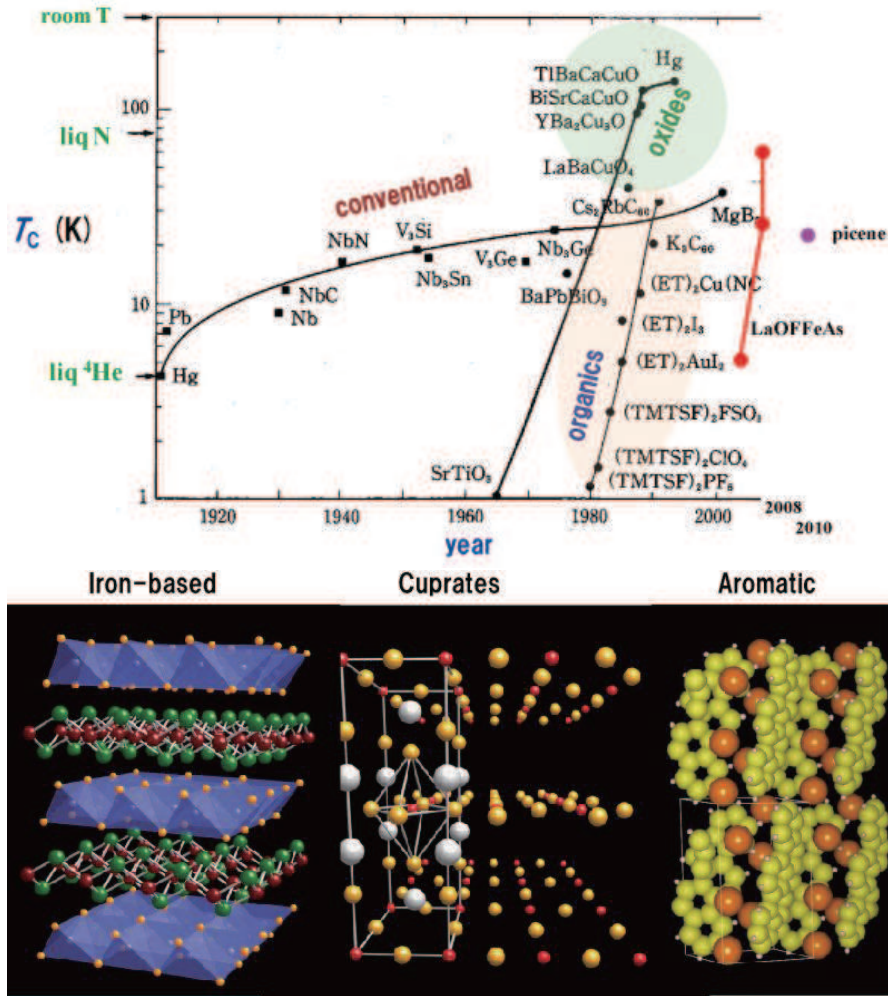


FIG. 1: (Top) T_c plotted against calendar year for various classes of superconductors. (Bottom) Typical crystal structures of the iron-based, cuprate and aromatic superconductors.

In the history of superconductivity, the conventional and intermetallic compounds were

followed by the oxide superconductors, which culminated in the cuprates in the 1980's. On the other hand, 1980 witnessed a discovery of an organic superconductor(SC), and the carbon-based SC subsequently attained a discovery of fullerene SC. 2008 marked the discovery of the iron-based SC,[7] the first non-copper SC with T_C exceeding 50 K. The most recent and important addition to the organic SC is an aromatic superconductivity discovered in 2010 in K-doped picene with $T_C \simeq 20$ K.[8] So the spectrum of SC materials ranges from the light-element, p-electron systems (MgB_2 , carbon-based, organic, etc) to transition-metal compounds (cuprates, cobaltates, iron-based, etc) down to higher-d-electron and f-electron systems (ruthenates, Hf compounds, heavy-fermion compounds, etc).

From the viewpoint of electron mechanism of SC, an interest is the way in which magnetism and superconductivity appear in correlated electron systems, which should be sensitive to the factors:

1. underlying band structure and the associated Fermi surface,
2. spatial dimensionality, and
3. orbital degrees of freedom.

We can even envisage a materials design by manipulating these factors[9]. First, the electronic structure is naturally governed by crystal structures. For the dimensionality, Arita et al[10] have shown, with the fluctuation exchange approximation, that 2D (layered) systems are generally more favourable for the spin-fluctuation-mediated SC than in 3D systems. The reason is traced back to the fact that the spin-fluctuation-mediated pairing interaction is appreciable only around localised regions in \mathbf{k} -space (unlike the phonon-mediated case), where the height and width of the susceptibility structures both in the frequency (ω) and momentum (\mathbf{q}) sectors turn out to be similar between 2D and 3D. This means that their *phase volume fraction* is much greater in 2D, and gives higher T_C in Éliashberg's equation. This agrees with the empirical fact that almost all the recently discovered SC (cuprates, Co compound, iron-based, Hf compound, CeCoIn_5 , solid picene, etc) are indeed layer-structured.

A second observation is that important classes of superconductors such as the iron-based are often inherently multiband systems. We shall show that the aromatic SC also has multiband structure derived from (nearly) degenerate molecular orbitals. So are the superconducting fullerenes. MgB_2 is another multiband system, comprising π and σ bands. Moreover,

we shall show that even the (single-layer) cuprates, usually regarded as a prototypical single-band system, can only be understood in terms of a two-band ($dx^2 - y^2, dz^2$) picture if we want to understand their material dependence. Thus all the important superconductors are in fact multiband systems. Historically, multiband SC was theoretically considered back in the 1950's and 60's by Suhl et al and by Kondo, so it has a long history, but we should definitely revisit the physics afresh in view of the new classes of superconductors. In other words, multibands provide an important *internal degree of freedom* dominating the system, which reminds us of the hyperfine states playing an important role in cold atoms.

For each of all the three classes of materials we first construct an electronic model with the “downfolding” based on first-principles electronic structure calculations. The pairing from repulsive interactions can be explained simply as anisotropic Cooper pairs accompanied by an anisotropic gap functions, $\Delta(\mathbf{k})$. In the BCS gap equation,

$$\Delta(\mathbf{k}) = - \sum_{\mathbf{k}'} V(\mathbf{k}, \mathbf{k}') \frac{\Delta(\mathbf{k}')}{2E(\mathbf{k}')} \tanh \left(\frac{E(\mathbf{k}')}{2k_B T} \right), \quad (1)$$

where $V(\mathbf{k}, \mathbf{k}')$ is the pairing interaction, we can immediately recognise that a repulsion acts as an attraction when $\Delta(\mathbf{k})$ changes sign across the typical momentum transfer (usually dictated by the nesting vectors that give spin fluctuation mode as is the case with the cuprate with an AF fluctuation producing a *d*-wave pairing). One intriguing point emerging from the relation of pairing with electronic structure is that the idea of “disconnected Fermi surface”[11] is often at work. Namely, if the Fermi surface comprises pockets or sheets with the major nesting vector between the disconnected elements, we can realise a pairing in which *each pocket is fully gapped with a sign reversal in the gap function* between the pockets. This is the basic idea of the disconnected Fermi surface, and gives an interesting avenue for realising high Tc superconductivity.

IRON-BASED SUPERCONDUCTORS

The iron-based superconductor[7] is a multi-d-band system as revealed from a microscopic model construction[2, 12]. A pairing symmetry, sign-reversing but nodeless $g_{\pm} \pm h$ where each Fermi pocket is fully gapped while different pockets have opposite signs, is suggested from the viewpoint of the spin-fluctuation mediated pairing. Thus, while an initial surprise on the iron-based pnictide as to why the major constituent, iron, which is an element

usually associated with magnetism, we can understand that iron, a transition metal element situated in the middle of the periodic table, is characterised by multiband structures for its compounds (Fig.2).

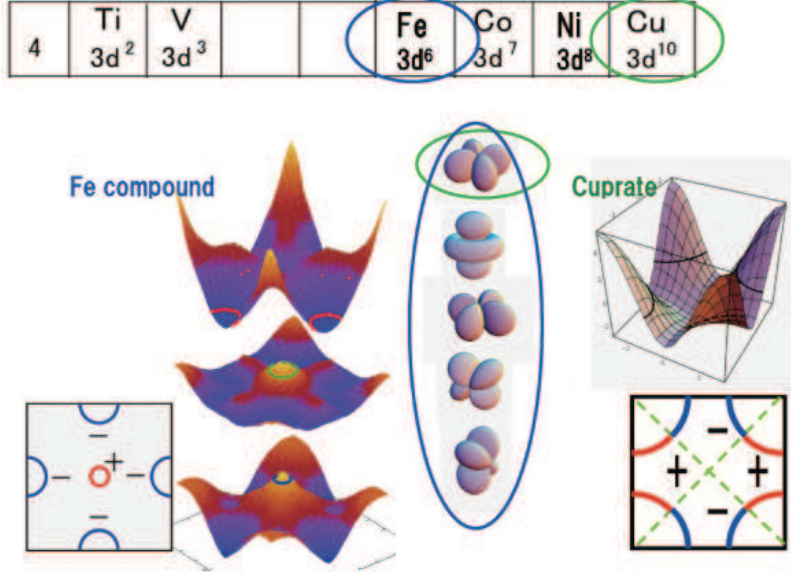


FIG. 2: Band dispersions and Fermi surfaces are schematically shown for the cuprate and iron-based superconductors, along with five d-orbitals.

The electronic structure calculation shows that three bands intersect E_F , and are primarily involved in the gap function, but actually all the five bands are *heavily entangled*, which reflects hybridisation of the five 3d orbitals due to the tetrahedral coordination of As 4p orbitals around Fe (Fig.1). Hence we conclude that the minimal electronic model requires all the five bands. The Fermi surface comprises two concentric hole pockets (α_1, α_2) centred around $(k_x, k_y) = (0, 0)$ and two electron pockets around $(\pi, 0)$ (β_1) and $(0, \pi)$ (β_2). In addition, a portion of the band near $(\pm\pi, \pm\pi)$ is flat and close to E_F around $n = 6.1$, so that the portion acts as a “quasi Fermi surface (γ)” around (π, π) .

We then apply the five-band random-phase approximation (RPA) to solve the Éliashberg equation. We conclude that a nesting between multiple Fermi surfaces (pockets) results in the unconventional $s\pm$ pairing[2]. Subsequently there have been a body of experimental results for identifying the pairing symmetry, and they primarily support $s\pm$, clearest of which is a phase-sensitive Fourier-transform STM spectroscopy[13], but exhibit significant material dependence within the iron-based compounds.

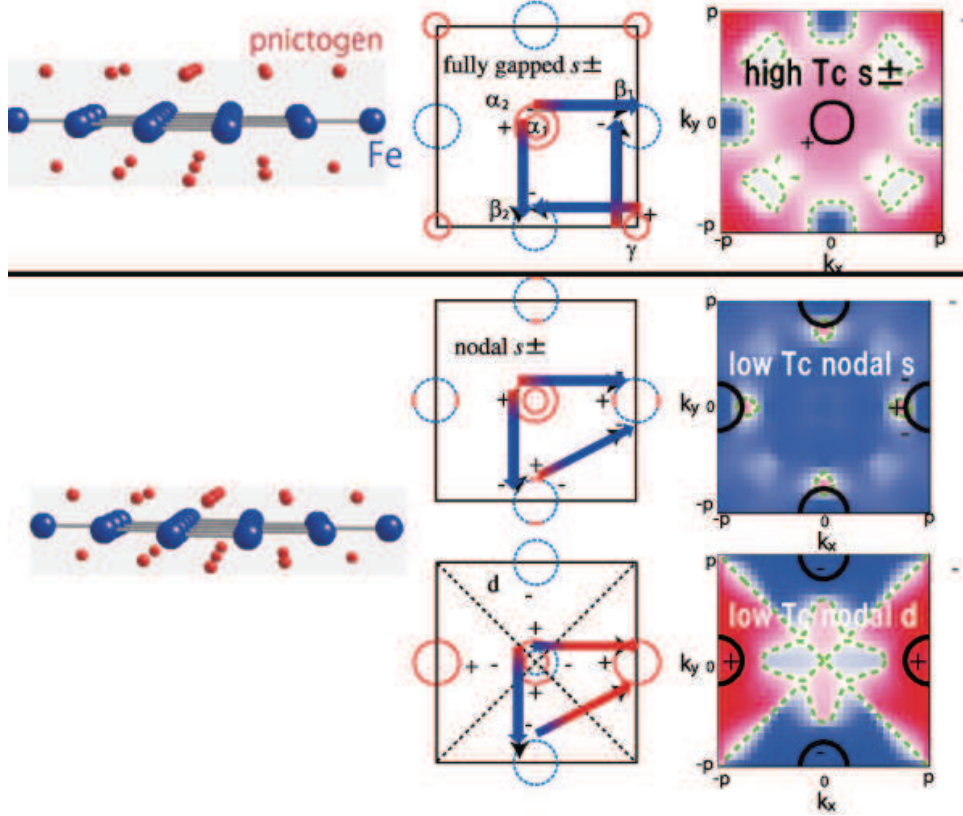


FIG. 3: Typical Fermi surfaces along with nesting vectors (middle column) and the gap functions (right) for higher (top) or lower (bottom) pnictogen heights.[3]

Indeed, a subtlety about multiband systems appears here as a sensitive dependence of the pairing on materials, as revealed in terms of “pnictogen height” [3] (Fig.3). The essence is that as the height is raised (e.g., as we go from LaFePO to LaFeAsO or NdFeAsO), the multibands deform and the $X^2 - Y^2$ band is shifted above E_F with a new pocket emerging around $(k_x, k_y) = (\pi, \pi)$. This changes the orbital character of the Fermi pocket and even the number of pockets. As a result, LaFeAsO and NdFeAsO are happy with the $s\pm$ pairing, while LaFePO has multiple nesting vectors that are frustrated, resulting in either nodal s or d -wave pairing.

This line of approach also explains the “Lee plot” [14], which indicates experimentally that T_C attains a maximum when the Fe-pnictogen tetrahedron approaches a regular tetrahedron. Usui and Kuroki [15] explain this as a maximised Fermi surface multiplicity optimising SC in iron pnictides, where we have a maximum number of pockets (two hole pockets and one hole pocket) for the regular tetrahedron. Impurity effects on SC should also be sensitive to

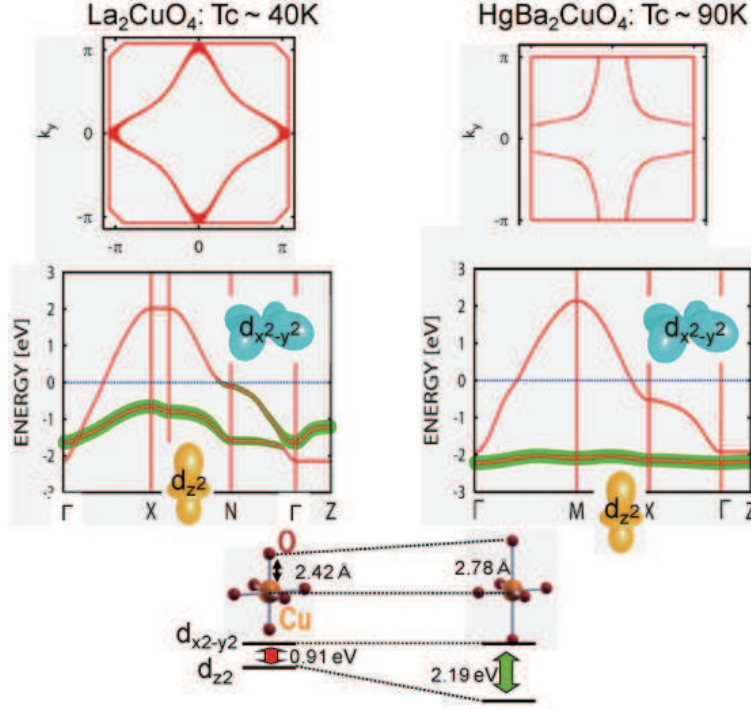


FIG. 4: Fermi surfaces (top) and band structures (middle, thickness representing the weight of dz^2 character) and the oxygen heights (bottom) are shown for La_2CuO_4 (left) and $\text{HgBa}_2\text{CuO}_4$ (right).[1]

multiband structure[16].

CUPRATE SUPERCONDUCTORS

Now, we can revisit the cuprate afresh, which has conventionally been viewed as a single($dx^2 - y^2$)-band system. This comes from copper being an element situated in the right end of the transition-metal periodic table. A single-band structure is in fact rather rare and almost miraculous. Let us start from a long-standing puzzle — why the single-layered cuprates, $\text{La}_{2-x}(\text{Sr}/\text{Ba})_x\text{CuO}_4$ ($T_C \simeq 40\text{K}$) and $\text{HgBa}_2\text{CuO}_{4+\delta}$ ($T_C \simeq 90\text{K}$), have such a significant difference in T_C ? The La system has a diamond-shaped Fermi surface with a relatively better nesting, while the Hg system has a warped Fermi surface with a poorer nesting, so that this sharply contradicts with a general view that better the nesting higher the T_C . Thus it is imperative to resolve this discrepancy if one wants to understand the curates.

We have revealed[1] that it is crucial to introduce a two-orbital model that explicitly incorporates the dz^2 orbital on top of the $dx^2 - y^2$ (Fig.4). The former component has in fact a significant contribution to the Fermi surface in the La system, which comes from a key parameter, the energy level difference, ΔE , between the $dx^2 - y^2$ and dz^2 orbitals. A smaller ΔE in the La system results in simultaneously a larger dz^2 hybridisation on the Fermi surface and a smaller second-neighbour hopping t_2 (hence a diamond-shaped Fermi surface). We have revealed that the degradation of superconductivity due to dz^2 hybridisation is so significant as to supersede the effect of the diamond-shaped (better-nested) Fermi surface. This resolves the long-standing puzzle. Conversely, we can predict that materials, if any, that have smaller t_2 with the single-band nature preserved will realise even higher T_C .

While in Ref.[1] the oxygen height above the CuO_2 plane is revealed to be a main factor, there exist in fact other factors.[17] To be more precise, the energy difference ΔE between the $d_{x^2-y^2}$ and d_{z^2} orbitals is the key parameter that governs both the hybridisation and the shape of the Fermi surface. A smaller ΔE tends to suppress T_c through a larger hybridisation, and vice versa. Then the question is what determines the material and lattice-structure dependence of ΔE . This is shown to be determined by the energy difference ΔE_d between the two $\text{Cu}3d$ orbitals (primarily governed by the apical oxygen height), and the energy difference ΔE_p between the in-plane and apical oxygens (primarily governed by the interlayer separation d).

When the doping is controlled by excess or vacancy oxygen atoms, there is an important question of how the local change in the crystal symmetry caused by these oxygens affect the electronic structure and T_c , as has been discussed in Ref.[18] In particular, local lattice distortions will hybridise different orbitals, as observed by EXAFS for lattice misfits in multilayer superconductors.[18] In the present paper we have discussed how the material and lattice structure determine the way in which the orbitals are hybridised over the whole crystal, while the hybridisation occurs locally for local distortions. So a possible relation of the effects of apical and in-plane oxygen atoms as revealed here to the effects of local oxygen configurations may be an interesting future problem.

Incidentally, effects of electron correlation appear in a variety of ways. For instance, the evolution of the Fermi surface with pocket-like shapes as observed in the cuprates in ARPES experiments have theoretically been discussed in terms of the Green's function for the correlated system, in a weak-coupling scheme[19] and in the cluster extension of the

dynamical mean-field theory[20].

AROMATIC SUPERCONDUCTORS

More recently, an organic superconductivity was discovered in potassium-doped solid picene, which is the first aromatic superconductor with transition temperatures $T_C = 7 - 20$ K[8]. The discovery came as a surprise, since aromatic molecules are most typical, textbook organic compounds, which have been certainly not associated with SC. The structure is a stack of layers, with each layer being a herringbone arrangement of picene molecules.

We have obtained a first-principles electronic structure of solid picene as a first step towards the elucidation of the mechanism of the superconductivity[5, 6]. The undoped crystal is found to have four conduction bands, which derive from LUMO (lowest unoccupied molecular orbital) and LUMO+1 of an isolated picene molecule, as revealed in terms of maximally localized Wannier orbitals. Since there are two molecules per unit cell of the herringbone, we have four bands, which are actually entangled due to a hybridisation of the LUMO and (LUMO+1).

For the K-doped systems, the bands are shown to be not rigid for two-fold reasons (i.e., a distorted herringbone structure upon doping along with a spilling of the molecular wave function over to potassium sites). The Fermi surface for K_3 picene is a curious composite of a warped two-dimensional surface and a three-dimensional one (Fig.5).

Kubozono’s group has also reported superconductivity in another aromatic molecule, coronene, with K-doping[21]. Motivated by this we have also obtained the first-principles electronic structure of solid coronene (Fig.5). In the undoped coronene crystal, the conduction band again comprises four bands, which originate from LUMO (doubly-degenerate, reflecting a higher symmetry of the molecule) and entangled as in solid picene. The Fermi surface for a candidate of the structure of K_x coronene with $x = 3$, for which superconductivity is found, comprises multiple sheets, as in doped picene but exhibiting a larger anisotropy with different topology.

As for SC, in a phonon mechanism the problem becomes the coupling between the electrons on such a Fermi surface and the molecular phonons. The situation gives an interesting possibility for electron mechanisms as well, since the nesting between multiple Fermi surfaces can give rise to a unique opportunity for an electron mechanism, especially in multiband

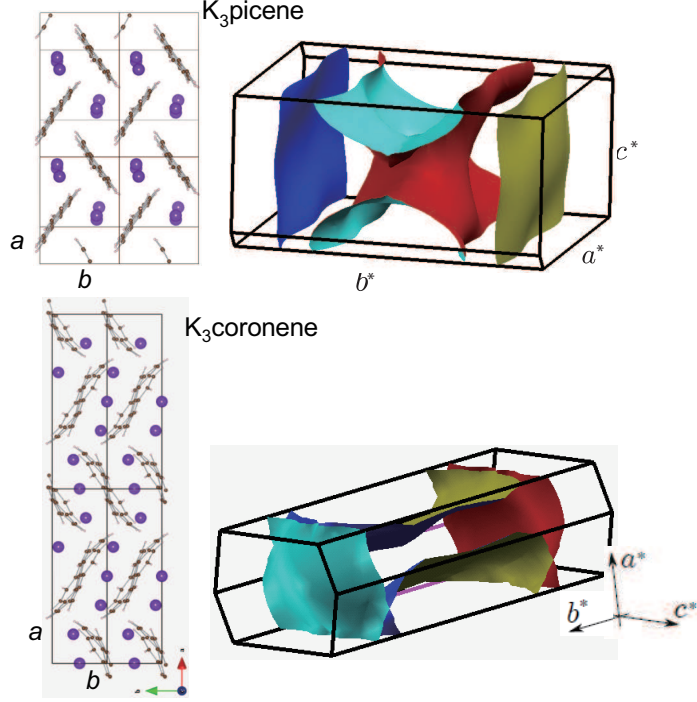


FIG. 5: Crystal structures (left) and Fermi surfaces (right) are shown for $K_3\text{picene}$ (top) and $K_3\text{coronene}$ (bottom).[5, 6]

cases.[9] One might wonder whether aromatic systems can be strongly correlated, but a possibility of Mott transition has been discussed for $K_x\text{pentacene}$ [22]

DISCUSSIONS AND SUMMARY

Thus all of iron, cuprate and aromatic superconductors have to be conceived as multiband systems, with some important differences among them. There are a host of other physical properties that are relevant to multiband systems. These include (i) collective (phase) modes in multiband SC which become unstable when three (or more) bands are frustrated[23], and (ii) spin Hall effect in multiband systems[24]. One important factor is the relevant energy scale in the pairing mechanism (e.g., the energy scale of the spin-fluctuation) for various classes of materials. These observations should give a renewed perspective on how superconductivity can dramatically depend on elements/crystal structures. In a completely different avenue, we can also explore non-equilibrium SC[25]. These will provide guiding principles for searching new high-Tc superconductivity for the decades to come.

The work described here is a collaboration with Kazuhiko Kuroki, Seiichiro Onari, Ryotaro Arita, Hidetomo Usui, Yukio Tanaka, Hiroshi Kontani, Hirofumi Sakakibara, Taichi Kosugi, Takashi Miyake, Shoji Ishibashi. This study has been supported in part by Grants-in-Aid for Scientific Research from MEXT of Japan, and from JST-TRIP.

- [1] H. Sakakibara, H. Usui, K. Kuroki, R. Arita and H. Aoki, Phys. Rev. Lett. **105**, 057003 (2010).
- [2] K. Kuroki, S. Onari, R. Arita, H. Usui, Y. Tanaka, H. Kontani, H. Aoki, Phys. Rev. Lett. **101** (2008) 087004; **102**, 109902(E) (2009).
- [3] K. Kuroki, H. Usui, S. Onari, R. Arita and H. Aoki, Phys. Rev. B **79**, 224511 (2009).
- [4] K. Kuroki et al, New J. Phys. **11**, 025017 (2009); H. Aoki, Physica C **469**, 890 (2009).
- [5] T. Kosugi, T. Miyake, S. Ishibashi, R. Arita and H. Aoki, J. Phys. Soc. Jpn **78**, 113704 (2009); Phys. Rev. B **84**, 214506 (2011).
- [6] T. Kosugi et al, Phys. Rev. B (R) **84**, 020507(R) (2011).
- [7] Y. Kamihara, T. Watanabe, M. Hirano, H. Hosono: J. Am. Chem. Soc. **130** (2008) 3296; H. Takahashi, K. Igawa, K. Arii, Y. Kamihara, M. Hirano, H. Hosono: Nature **453** (2008) 376.
- [8] R. Mitsuhashi et al, Nature **464**, 76 (2010).
- [9] H. Aoki, Physica C **437-438**, 11 (2006); H Aoki in *Condensed Matter Theories* **21** ed. by H. Akai et al, (Nova Science, 2007).
- [10] R. Arita, K. Kuroki, H. Aoki: Phys. Rev. B **60** (1999) 14585; P. Monthoux, G. G. Lonzarich, Phys. Rev. B **59** (1999) 14598.
- [11] K. Kuroki, R. Arita: Phys. Rev. B **64** (2001) 024501; Phys. Rev. B **66** (2002) 184508.
- [12] I. I. Mazin, D. J. Singh, M. D. Johannes and M. H. Du, Phys. Rev. Lett. **101** (2008) 057003.
- [13] T. Hanaguri et al, Science **323**, 923 (2009); T. Hanaguri et al, Science **328**, 474 (2010).
- [14] C.-H. Lee et al, J. Phys. Soc. Jpn **77**, 083704 (2008).
- [15] H. Usui and K. Kuroki, Phys. Rev. B **84**, 024505 (2011).
- [16] Y. Nagai, K. Kuroki, M. Machida and H. Aoki, arXiv:1012.5565.
- [17] H. Sakakibara, H. Usui, K. Kuroki, R. Arita and H. Aoki, Phys. Rev. B **85**, 064501 (2012).
- [18] A. Bianconi et al, J. Phys.: Condens. Matter **12**, 10655 (2000); N. Poccia, A. Ricci and A. Bianconi, *Advances in Condensed Matter Physics* doi:10.1155/2010/261849 (2010); N. Poccia

- et al, nature materials **10**, 733 (2011).
- [19] T. M. Rice, K.-Y. Yang and F. C. Zhang, Rep. Prog. Phys. **75**, 016502 (2012).
 - [20] S. Sakai, Y. Motome and M. Imada, Phys. Rev. Lett. **102**, 056404 (2009); Phys. Rev. B **82**, 134505 (2010).
 - [21] Y. Kubozono et al, Phys. Chem. Chem. Phys. **13**, 16476 (2011).
 - [22] M. F. Craciun et al, Phys. Rev. B **79**, 125116 (2009).
 - [23] Y. Ota, M. Machida, T. Koyama and H. Aoki, Phys. Rev. B **83**, 060507(R) (2011).
 - [24] S. Pandey, H. Kontani, D. S. Hirashima, R. Arita and H. Aoki, arXiv:1107.0122.
 - [25] N. Tsuji, T. Oka, P. Werner and H. Aoki, Phys. Rev. Lett. **106**, 236401 (2011); arXiv:1110.2925.